

**This version of the ESI replaces the previous version published on 02.04.2024 to correct the information displayed in Figure S4.**

## Supporting information

### **Plasma-catalytic One-Step Steam Reforming of CH<sub>4</sub> to CH<sub>3</sub>OH and H<sub>2</sub> promoted by Oligomerized [Cu-O-Cu] Species on Zeolites**

Wei Fang,<sup>1</sup> Ximiao Wang,<sup>1</sup> Shangkun Li,<sup>1,2</sup> Yingzi Hao,<sup>1</sup> Yuping Yang,<sup>1</sup> Wenping Zhao,<sup>3</sup> Rui Liu,<sup>1</sup> Dongxing Li,<sup>1</sup> Chuang Li,<sup>1</sup> Xiaoxia Gao,<sup>4</sup> Li Wang,<sup>5</sup> Hongchen Guo,<sup>1</sup> Yanhui Yi\*<sup>1</sup>

<sup>1</sup> State Key Laboratory of Fine Chemicals, Frontier Science Center for Smart Materials, School of Chemical Engineering, Dalian University of Technology, Dalian 116024, P.R. China.

<sup>2</sup> Research group PLASMANT, Department of Chemistry, University of Antwerp, Universiteitsplein 1, BE-2610 Wilrijk-Antwerp, Belgium.

<sup>3</sup> China Tianchen Engineering Corporation, Tianjin, 300409, P.R. China.

<sup>4</sup> Instrumental Analysis Center, Dalian University of Technology, Dalian, 116024, P.R. China.

<sup>5</sup> College of Environmental Sciences and Engineering, Dalian Maritime University, Dalian 116026, Liaoning, China

Email: yiyanhui@dlut.edu.cn

## Table of Contents

1. Catalyst preparation
2. Experimental setup (Scheme S1)
3. Catalytic tests
4. Product analysis (Figure S1, Table S1)
5. Catalytic performances (Figure S2, Figure S3)
6. Electric parameters of the DBD (Figure S4)
7. Comparison of this work with literature results (Table S2)
8. Catalyst characterization (Table S3, Figure S5, Figure S6, Figure S7)
9. Comparison of the Cu/MOR catalysts with Cu/SiO<sub>2</sub> catalysts (Figure S8)
10. *In-situ* FTIR (Scheme S2, Figure S9)
11. Characterization of the spent catalysts (Figure S10, Figure S11)
12. *In-situ* Optical emission spectra

## 1 Catalyst preparation

The MOR zeolite was prepared as follows. 1.53 g NaOH was dissolved into 46 g H<sub>2</sub>O, and then 14.71 g tetraethyl ether ammonium hydroxide (TEAOH, 25 wt %), 0.99 g NaAlO<sub>2</sub> and 30 g silica sol (SiO<sub>2</sub>, 30 wt %) were added in turn. After 4 h stirring and aging, the mixture was transferred into a 100 mL autoclave lined with PTFE and heated at 170 °C for 3 day under static and atmospheric pressure. After that, the sample was filtered and washed with water until neutral PH value. Then, the sample was dried overnight in an oven at 110 °C, and calcined in a muffle furnace at 540 °C (heating rate 1°C/min) to remove the organic template agent and other impurities. Finally, we obtained Na/MOR zeolite with a Si/Al ratio of 25.

The H/MOR zeolite was prepared from Na/MOR as follows. 1 g Na/MOR zeolite was added into 20 mL NH<sub>4</sub>NO<sub>3</sub> solution (1 mol/L<sup>-1</sup>), and then the mixture was stirred for 6 h at 80 °C (controlled by a water bath). After washing with deionized water, and the resulting precursor was filtered and reprocessed in the same manner for a total of 2 times. Then the sample was dried at 100 °C for 12 h. Finally, the H/MOR was obtained by calcination at 500 °C for 5 h.

To prepare Cu/MOR catalyst, Cu ion exchange was performed as follows. 2 g H/MOR was added into 4.8 mL Cu(NO<sub>3</sub>)<sub>2</sub>·3 H<sub>2</sub>O solution (0.4 mol/L<sup>-1</sup>), and then the mixture was stirred for 2 h at 90 °C. The mixture was then filtered, washed with deionized water and dried overnight in an oven at 100°C. Repeat the process three times in the same manner. The obtained samples were calcined under the same conditions as the H/MOR samples to obtain the final Cu/MOR catalyst. H/ZSM-5, MCM-41 and H/Beta zeolites were purchased from Nankai University Catalyst Co., Ltd. Cu/ZSM-5, Cu/MCM-41 and Cu/Beta zeolites were prepared using the same preparation method as the Cu/MOR zeolite.

Cu/MOR and Cu/SiO<sub>2</sub> catalysts were also prepared by an impregnation method (IM) with fumed SiO<sub>2</sub> and H/MOR as supports. Taking the preparation of Cu/SiO<sub>2</sub> catalyst with 10 wt.% loading as an example, 4.15 g Cu(NO<sub>3</sub>)<sub>2</sub>·3H<sub>2</sub>O sample (calculated according to 10 wt.% loading) was dissolved into 20 ml deionized water, and 10 g fumed SiO<sub>2</sub> was added into the mixture. After full stirring and aging for 12 h at room temperature, the sample was dried overnight in an oven at 120 °C. The sample was then calcined in a muffle furnace at 540 °C for 5 h to obtain the final Cu/SiO<sub>2</sub> catalyst.

Finally, the prepared catalyst powders were pressed and shaped into sieves (20-40 mesh) for plasma-catalytic reactions.

## 2 Experimental setup

A coaxial DBD reactor (Scheme S1) was used to generate non-thermal plasma. A stainless steel with a diameter of 2 mm is inserted inside the quartz tube as a high voltage electrode, and outside the quartz tube, the upper section of the sieve plate is wrapped with a wire with a 30 mm long aluminum foil as the plasma discharge zone, as well as a thermocouple to monitor the temperature of the discharge zone in real time, and another wire is taken as a grounding electrode. The discharge zone is filled with 1.2 g of catalyst (20-40 mesh).

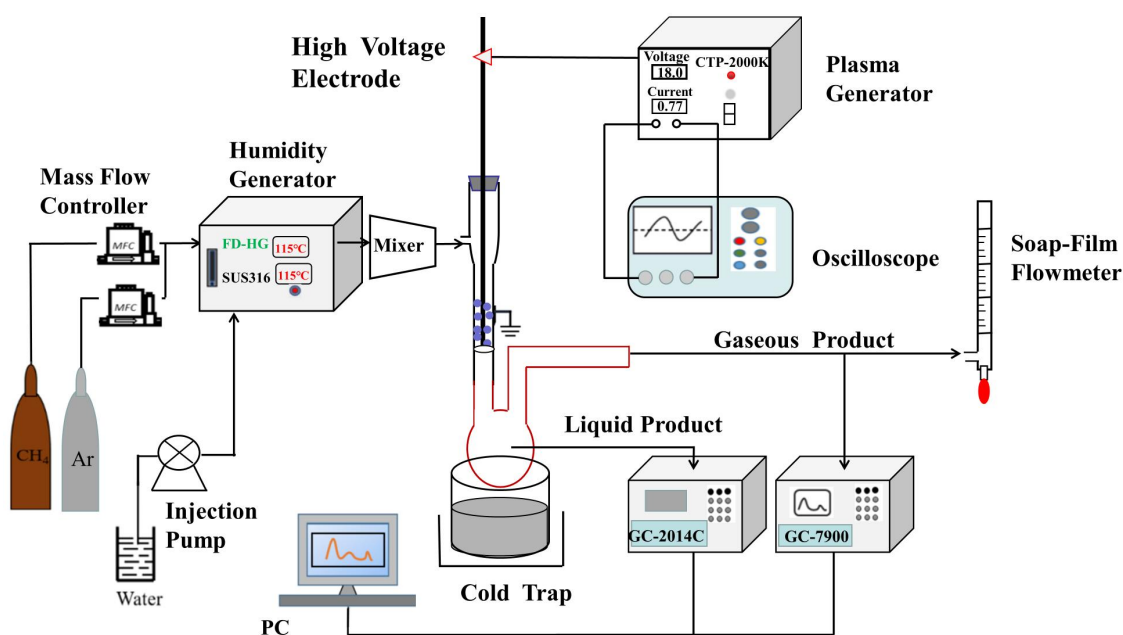
Water vapor (80 ml/min) was supplied by a steam generator (FD-HG from fad laboratory equipment Co., Ltd.) at 115 °C vaporization temperature, and the flow rate of water vapor was controlled by an injection pump. CH<sub>4</sub> (20 ml/min) and Ar (40 ml/min) were monitored by mass flow controllers, and the three gases were homogeneously mixed before passing through the plasma reactor. There are two caveats to the experiments.

Firstly, the gas line must be heated with a heating ribbon to avoid condensation of the water vapor. Because liquid state of water not only leads to non-uniformity mixing of CH<sub>4</sub> and H<sub>2</sub>O, being conducive to C-C coupling reaction of CH<sub>4</sub> for C<sub>2</sub>H<sub>6</sub> production in partial space of the reactor with abundant CH<sub>4</sub> but scarce H<sub>2</sub>O, but also results in shortage of heat in the fixed-bed to drive the endothermic OSRMtM reaction since the vaporization of liquid water in the discharge zone consumes a lot of heat. To avoid the above mentioned problems in this study, we used a steam generator to supply water vapor, which was homogeneously mixed with CH<sub>4</sub> and Ar before passing through the plasma reactor. In addition, the gas line was heated with a heating ribbon, and the temperature was maintained at 115 °C to avoid condensation of the water vapor.

Secondly, noble gases (Ar) was added into the feed stock to improve the discharge through Penning ionization. Generally, DBD discharge is inhibited by electron affinity of H<sub>2</sub>O molecules, which is not favorable for activation of H<sub>2</sub>O molecules. Thus OSRMtM was relatively inhibited but C-C coupling reaction of CH<sub>4</sub> for C<sub>2</sub>H<sub>6</sub> production was relatively enhanced when noble gas is absent. Therefore, in this paper, Ar was added into the feed stock to improve the DBD, and thus improve activation of H<sub>2</sub>O molecules for OSRMtM.

The gaseous products were analyzed by an on-line gas chromatograph (Tianmei GC-7900, TDX-01 column, alumina-filled column) equipped with a thermal conductivity detector (TCD) and a flame ionization detector (FID). The discharge frequency was fixed at 14.2 kHz and the discharge voltage was kept at about 2.5 kV. The discharge voltage and current were measured by a digital fluorescence oscilloscope (Tektronix, DPO 3012) with a high voltage probe (Tektronix P6015) and a current probe (Pearson 6585). Liquid products were collected by a cold trap (a mixture of isopropanol and liquid nitrogen at temperatures below -120 °C) and then analyzed by GC-2014C

(Shimadzu, polyethylene glycol-2000 column) and GC-MS (Agilent 5975C, DB-1701 column). GC-2014C instrument equipped with a FID was used to measure products species. A Durabond (DB-1) wax column with a polar substrate was used to support aqueous injections. The column was 320  $\mu\text{m}$  thick and 30 m long and installed in an oven. The GC temperature program was set to 40  $^{\circ}\text{C}$  at the time of injection followed by a linear ramp of 10  $^{\circ}\text{C}/\text{min}$  to 150  $^{\circ}\text{C}$  (2 min hold time) and a second linear ramp of 10  $^{\circ}\text{C}/\text{min}$  to 220  $^{\circ}\text{C}$  (15 mins hold time). Hydrogen was used as the carrier gas with a constant flow rate (1ml/min) and nitrogen was used as the make-up gas. A split/splitless inlet was used (50:1 split ratio) with an inlet pressure of 50 kPa and an inlet temperature of 220  $^{\circ}\text{C}$ . An inlet liner containing glass wool was used to ensure uniform vaporization of water. Unknown samples were analyzed with gas injection volumes of 100  $\mu\text{l}$  (using a Hamilton gas-tight 1700 series syringe with a cemented 22 gauge needle and point style 5 with a 1700 series chaney adapter to lower the uncertainty in gaseous injection to  $\sim 1\%$ ) and aqueous injections were 1  $\mu\text{l}$  to keep the column and the inlet from getting damaged.



**Scheme S1.** Experimental setup for the  $\text{CH}_4/\text{Ar}/\text{H}_2\text{O}$  plasma reaction.

### 3 Catalytic tests

To evaluate the reaction performance of the catalysts, the conversion of the reactants and the selectivity of the main products were calculated by the following equations.

The CH<sub>4</sub> conversion is calculated by the following equation:

$$X_{\text{CH}_4} (\%) = \frac{\text{moles of CH}_4 \text{ converted}}{\text{moles of inputted CH}_4} \times 100 \% \quad (1)$$

The selectivity of the gas product is calculated as:

$$S_{\text{CO}} (\%) = \frac{n_{\text{CO}}^{\text{outlet}}}{n_{\text{CH}_4}^{\text{inlet}} - n_{\text{CH}_4}^{\text{outlet}}} \times 100 \% \quad (2)$$

$$S_{\text{CO}_2} (\%) = \frac{n_{\text{CO}_2}^{\text{outlet}}}{n_{\text{CH}_4}^{\text{inlet}} - n_{\text{CH}_4}^{\text{outlet}}} \times 100 \% \quad (3)$$

$$S_{\text{C}_2\text{H}_6} (\%) = \frac{2n_{\text{C}_2\text{H}_6}^{\text{outlet}}}{n_{\text{CH}_4}^{\text{inlet}} - n_{\text{CH}_4}^{\text{outlet}}} \times 100 \% \quad (4)$$

$$S_{\text{C}_2\text{H}_4} (\%) = \frac{2n_{\text{C}_2\text{H}_4}^{\text{outlet}}}{n_{\text{CH}_4}^{\text{inlet}} - n_{\text{CH}_4}^{\text{outlet}}} \times 100 \% \quad (5)$$

$$S_{\text{C}_3\text{H}_8} (\%) = \frac{3n_{\text{C}_3\text{H}_8}^{\text{outlet}}}{n_{\text{CH}_4}^{\text{inlet}} - n_{\text{CH}_4}^{\text{outlet}}} \times 100 \% \quad (6)$$

The total selectivity of the liquid-phase products was calculated as:

$$\text{Total selectivity of liquid products } (\%) = 100\% - (S_{\text{CO}} + S_{\text{CO}_2} + S_{\text{C}_2\text{H}_6} + S_{\text{C}_2\text{H}_4} + S_{\text{C}_3\text{H}_8})$$

(7)

The formula for calculating the selectivity of the liquid-phase oxygen-containing compounds is:

$$S_{\text{C}_x\text{H}_y\text{O}_z} (\%) = \frac{X \times n_{\text{C}_x\text{H}_y\text{O}_z}}{n_{\text{CH}_3\text{OH}} + 2n_{\text{C}_2\text{H}_5\text{OH}} + 2n_{\text{CH}_3\text{CHO}} + 2n_{\text{CH}_3\text{COOH}}} \times [100\% - (S_{\text{CO}} +$$

$$S_{\text{CO}_2} + S_{\text{C}_2\text{H}_6} + S_{\text{C}_2\text{H}_4} + S_{\text{C}_3\text{H}_8})] \quad (8)$$

Where  $n_{\text{C}_x\text{H}_y\text{O}_z}$  represents the number of moles of various oxygenates in the liquid fraction. Furthermore, we determine the H<sub>2</sub>O conversion (9) based on the oxygen balance, followed by the calculation of H<sub>2</sub> selectivity (10).

$$X_{\text{H}_2\text{O}} (\%) = \frac{n_{\text{CO}}^{\text{outlet}} + z \times n_{\text{C}_x\text{H}_y\text{O}_z}^{\text{outlet}}}{n_{\text{H}_2\text{O}}^{\text{inlet}}} \times 100\% \quad (9)$$

$$S_{\text{H}_2} (\%) = \frac{2 \times n_{\text{H}_2}^{\text{outlet}}}{4 \times n_{\text{CH}_4}^{\text{inlet}} \times X_{\text{CH}_4} + 2 \times X_{\text{H}_2\text{O}} \times n_{\text{H}_2\text{O}}^{\text{inlet}}} \times 100\% \quad (10)$$

## 4 Product analysis

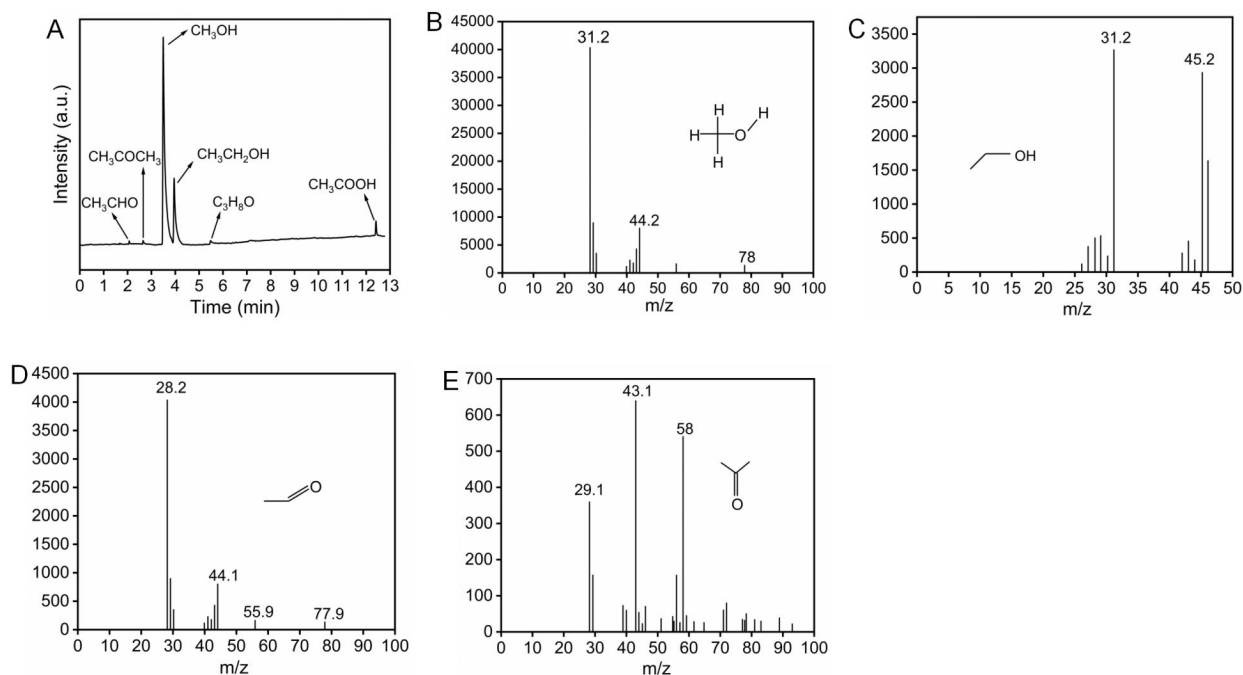


**Figure S1.** Qualitative analysis of liquid products. (A) GC profile indicating the presence of CH<sub>3</sub>OH, C<sub>2</sub>H<sub>5</sub>OH, CH<sub>3</sub>CHO, CH<sub>3</sub>COCH<sub>3</sub>, C<sub>3</sub>H<sub>8</sub>O, and CH<sub>3</sub>COOH, and GC-MS spectra of (B) CH<sub>3</sub>OH, (C) C<sub>2</sub>H<sub>5</sub>OH, (D) CH<sub>3</sub>CHO and (E) CH<sub>3</sub>COCH<sub>3</sub>.

**Table S1.** The standard curves for each substance is obtained by the external standard method.

Products	Analysis Method	Equation	Adj.R-Square
CH <sub>4</sub>	GC	Y=3968205.07X + 65036.71	0.999
C <sub>2</sub> H <sub>6</sub>	GC	Y =7451500X	0.999
C <sub>2</sub> H <sub>4</sub>	GC	Y =7.555180X	0.999
C <sub>3</sub> H <sub>8</sub>	GC	Y =16011374X	0.998
CH <sub>3</sub> OH	GC	Y=92704.4X	0.998
C <sub>2</sub> H <sub>5</sub> OH	GC	Y=118790X	0.998
CH <sub>3</sub> CHO	GC	Y=29678.5X	0.998
CH <sub>3</sub> COOH	GC	Y=49613.1X	0.999

Y denotes the peak area of the sample; X denotes the concentration of the sample in mol/L.

## 5 Catalytic performances

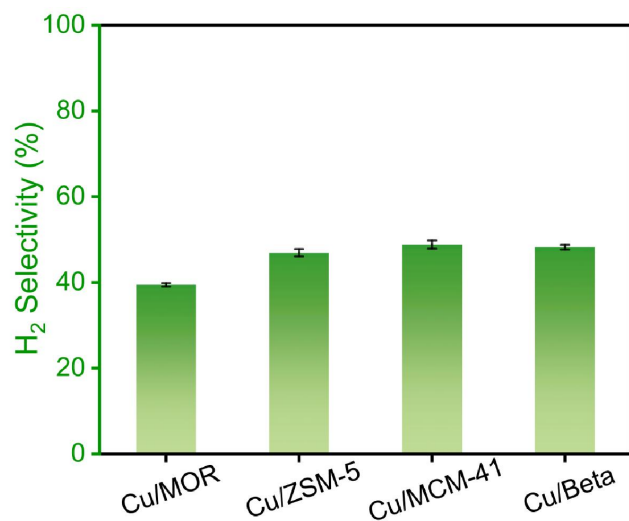


Figure S2. H<sub>2</sub> selectivity in plasma-catalytic OSRMtM using different catalysts.

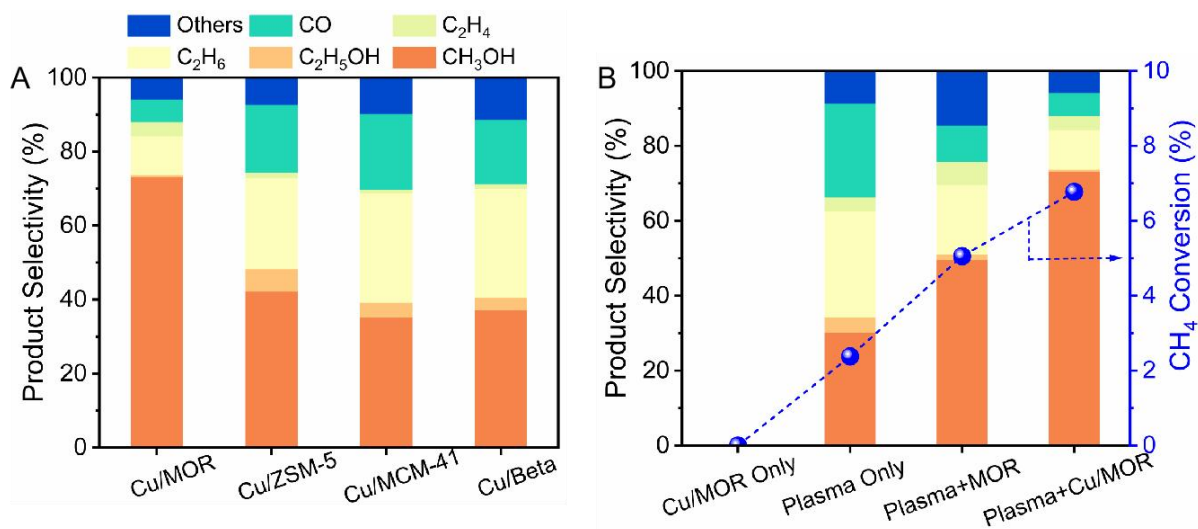
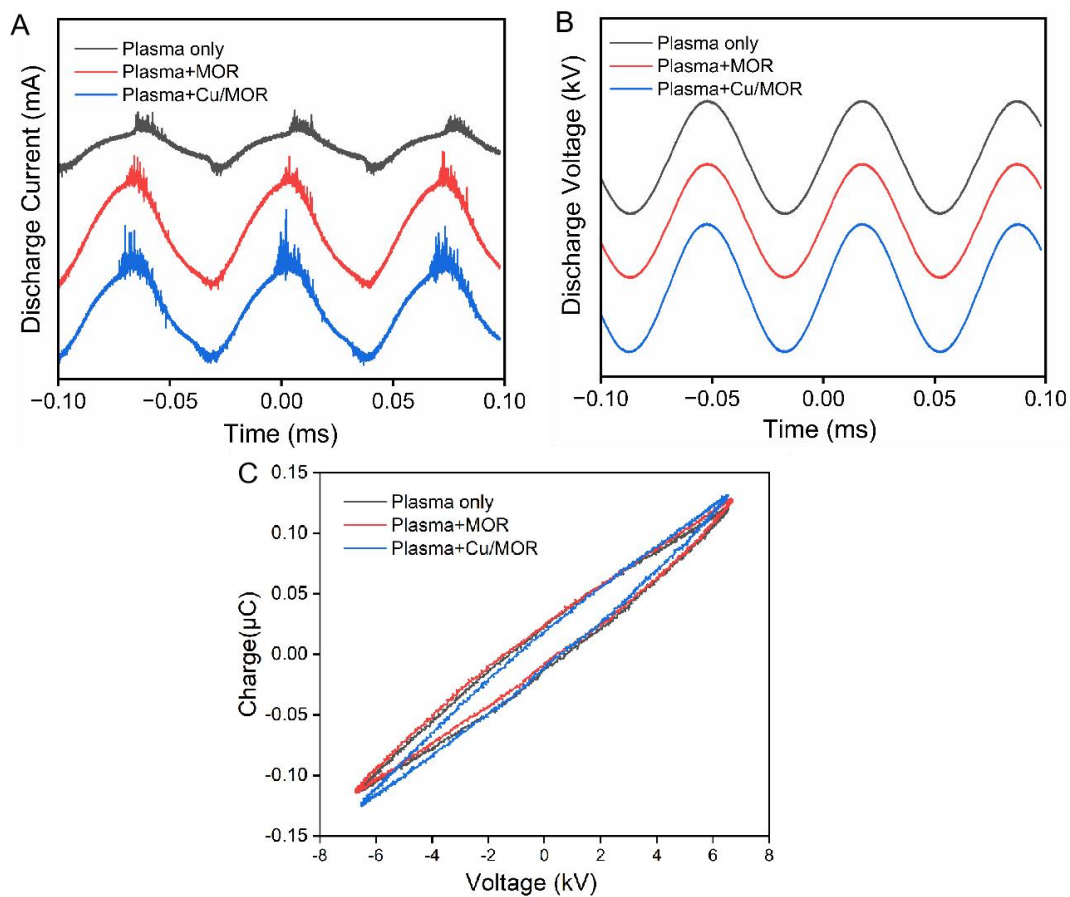


Figure S3. Products selectivity in the plasma-catalytic OSRMtM with (A) Cu/zeolite catalysts, (B) Different reaction modes.

## 6 Electric parameters of the DBD

An oscilloscope (Tektronix DPO 3012) with a high voltage probe (Tektronix P6015A) and a current probe (Pearson 6585) was used to collect the discharge voltages and discharge currents, as well as Lissajous figures (Figure S4).



**Figure S4.** Discharge parameters of the DBD. (A) Discharge current, (B) Discharge voltage, and (C) Lissajous figures.

## 7 Comparison of this work with literature results

Table S2. Comparative literature results of CH<sub>4</sub> to CH<sub>3</sub>OH in various plasma catalysis systems.

Plasma + catalyst in this paper					
Catalyst	CH <sub>4</sub> /Oxidant	Temp.(K)	Power(W)	CH <sub>4</sub> Conv.(%)	CH <sub>3</sub> OH Sel.(%)
Cu/MOR				6.8	73.1
Cu/ZSM-5	CH <sub>4</sub> :H <sub>2</sub> O=1:4	443	5	4.5	42.3
Cu/MCM-41				4.4	35.2
Cu/Beta				3.8	37.2
Plasma only from literature					
Catalyst	CH <sub>4</sub> /Oxidant	Temp.(K)	Power(W)	CH <sub>4</sub> Conv.(%)	CH <sub>3</sub> OH Sel.(%)
Plasma only <sup>1</sup>	CH <sub>4</sub> :H <sub>2</sub> O=3:1	393	/	1.067	7.5
Plasma only <sup>2</sup>	CH <sub>4</sub> :H <sub>2</sub> O=1:5	/	3	5	20
Plasma only <sup>3</sup>	CH <sub>4</sub> :O <sub>2</sub> =3:1	288	118	6	19
Plasma only <sup>4</sup>	CH <sub>4</sub> :O <sub>2</sub> =4:1	353	200	3	30
Plasma only <sup>5</sup>	CH <sub>4</sub> :N <sub>2</sub> O=1:1	<sup>a</sup> RT	0.27-7.7	5	43
Plasma + catalyst from literature					
Catalyst	CH <sub>4</sub> /Oxidant	Temp.(K)	Power(W)	CH <sub>4</sub> Conv.(%)	CH <sub>3</sub> OH Sel.(%)
Ni/SiO <sub>2</sub> <sup>6</sup>	CH <sub>4</sub> : H <sub>2</sub> O=1:2	673	56	13.1	/
TiO <sub>2</sub> <sup>7</sup>	CH <sub>4</sub> : H <sub>2</sub> O	308	30	/	93% (in liquid)
Cu/MOR <sup>8</sup>	CH <sub>4</sub> : H <sub>2</sub> O=1:3	393	7.7	2.16	30
Fe/γ-Al <sub>2</sub> O <sub>3</sub> <sup>9</sup>	CH <sub>4</sub> : O <sub>2</sub> =5:1	<sup>a</sup> RT	1.8	13	36
Ga/CZA <sup>10</sup>	CH <sub>4</sub> : O <sub>2</sub> =4:1	/	50	54.5	22.2
NiO/γ-Al <sub>2</sub> O <sub>3</sub> <sup>11</sup>	CH <sub>4</sub> : O <sub>2</sub> =2:1	353	30	6.4	50
Glass Beads <sup>12</sup>	CH <sub>4</sub> : O <sub>2</sub> =5:1	/	1.7	15.4	35.4
Cu-S-1 <sup>13</sup>	CH <sub>4</sub> : O <sub>2</sub> =4:1	293	15	5.8	50.6
Fe <sub>2</sub> O <sub>3</sub> /CuO/Al <sub>2</sub> O <sub>3</sub> <sup>14</sup>	CH <sub>4</sub> : Air=1:1	473	120	43	3.7
Fe <sub>2</sub> O <sub>3</sub> -CuO/CP <sup>15</sup>	CH <sub>4</sub> : Air=1:1	473	140	26	11
Cu-Ni/CeO <sub>2</sub> <sup>16</sup>	CH <sub>4</sub> : N <sub>2</sub> O=5:1	-	6	23	36

<sup>a</sup>RT: Room temperature.

## 8 Catalyst characterization

The crystal structure of the catalyst was analyzed by an X-ray diffractometer (XRD). The instrument model used is Rigaku D-Max 2400, using an Cu K $\alpha$  -ray source, tube pressure 40 kV, tube flow 25 mA, 2 $\theta$ , angular scanning range 5-80  $^{\circ}$ , scanning speed 10  $^{\circ}$ /min, with a step length of 0.02. The content of silicon, aluminum, and loaded copper in the four molecular sieves are measured through an X-ray fluorescence spectrometer (XRF).

N<sub>2</sub> physical adsorption is used to measure the specific surface area (inner and external surface area), pore capacity and pore distribution of the catalyst materials. The instrument used is a TriStar II 3020 produced by Micrometrics. Total surface area was obtained from the Brunauer-Emmett-Teller (BET) method. Micropore volume and supersurface area were obtained by t-plot.

H<sub>2</sub> program heating reduction (H<sub>2</sub>-TPR) was used to analyze the valence change of copper loaded on the surface of the catalyst. Weigh 0.15-0.2 g catalyst, blow out He gas at 550  $^{\circ}$ C for 1h before cooling to room temperature, then heat up from 100  $^{\circ}$ C to 800  $^{\circ}$ C in the H<sub>2</sub> atmosphere.

The analysis of elemental valence states and their changes in the catalysts was performed by X-ray photoelectron spectroscopy (XPS). The instrument used was a Thermo Fisher ESCALAB XI<sup>+</sup> model with an Al K $\alpha$ -ray light source. The binding energy was calibrated for all elements at C1s (284.8 eV). The valence state of Cu species on the surface of the metal catalysts was analyzed by ultraviolet-visible spectrophotometer (UV-Vis), using the instrument used was UV-550 UV spectrophotometer with integrating sphere attachment (built-in dra2500) from Agilent, USA, and the diffuse reflectance spectrum in the range of 190-900 nm was collected with BaSO<sub>4</sub> white plate as reference.

The particle dispersion and particle size of the loaded metal catalysts were analyzed by high-resolution transmission electron microscopy (HRTEM). The instrument used for HRTEM was a Tecnai G2 F30 S-Twin with an accelerating voltage of 300 kV.

**Table S3.** Composition and structural analysis of zeolites and Cu/zeolite.

Samples	SiO <sub>2</sub> /Al <sub>2</sub> O <sub>3</sub> ratio	Cu/Al ratio	Cu loading	S <sub>BET</sub> (m <sup>2</sup> ·g <sup>-1</sup> )	V <sub>micro</sub> (cm <sup>3</sup> ·g <sup>-1</sup> )	Pore Size (nm)
MOR	/	/	/	556	0.19	1.94
ZSM-5	/	/	/	402	0.13	1.77
MCM-41	/	/	/	570	0.17	4.40
Beta	/	/	/	585	0.17	2.86
Cu/MOR-fresh	18.81	0.22	2.25	517	0.18	1.91
Cu/ZSM-5-fresh	22.85	0.22	1.89	360	0.11	1.79
Cu/MCM-41-fresh	23.46	0.23	1.87	550	0.16	4.28
Cu/Beta-fresh	22.56	0.24	2.03	575	0.17	2.84

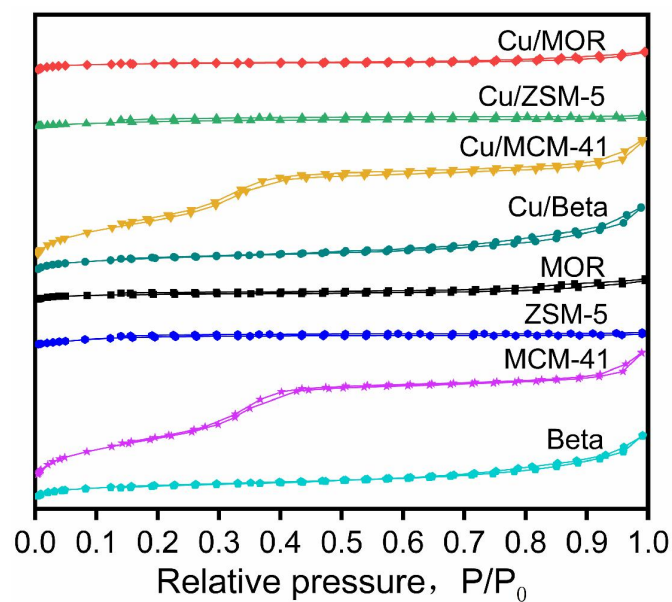


**Figure S5.** Nitrogen adsorption-desorption isotherms obtained at 77K for Cu/zeolite samples.

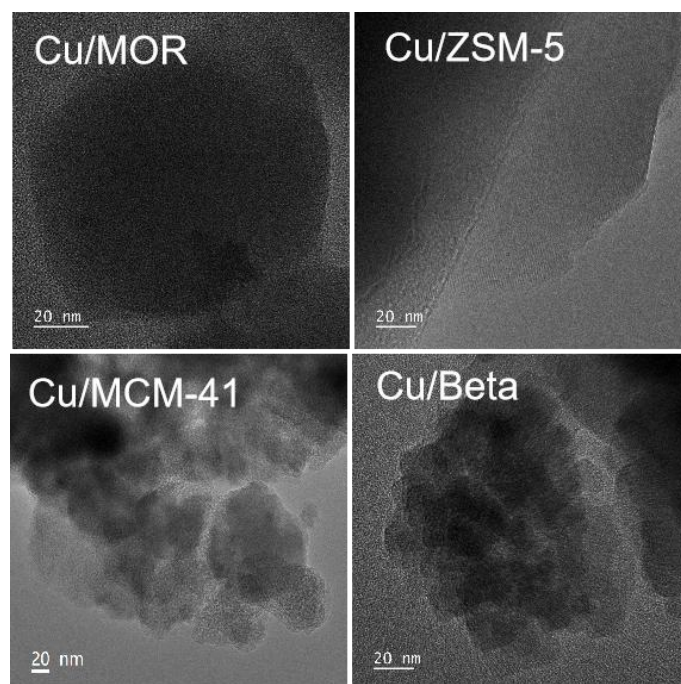


**Figure S6.** HRTEM images of the Cu/zeolite catalysts.

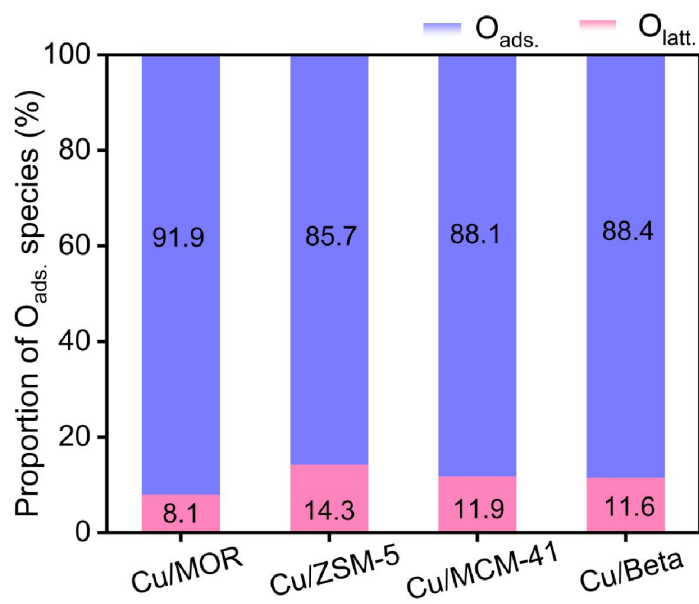


**Figure S7.** The proportion of different O species in the fresh Cu/zeolite samples.

## 9 Comparison of the Cu/MOR catalysts with Cu/SiO<sub>2</sub> catalysts

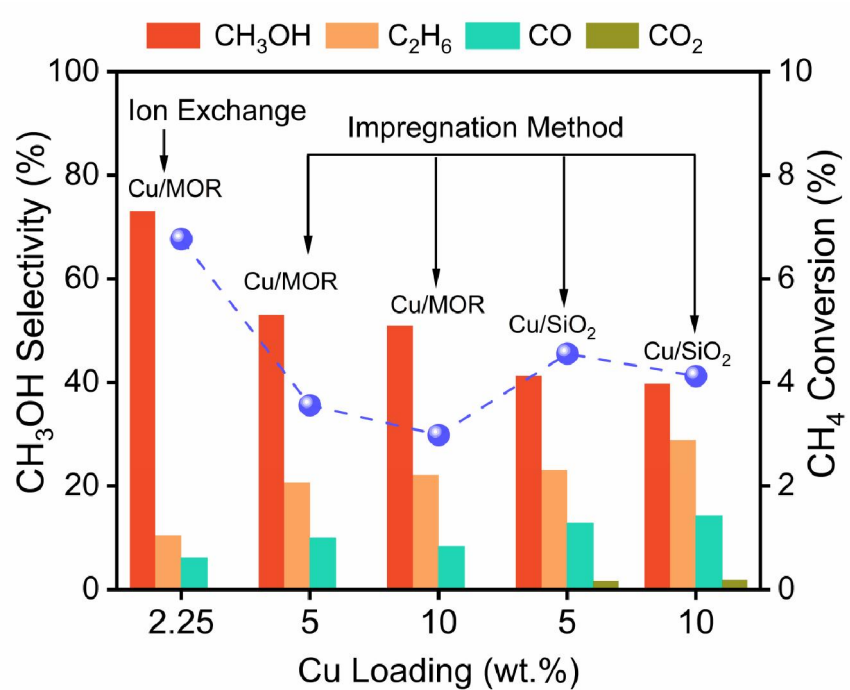
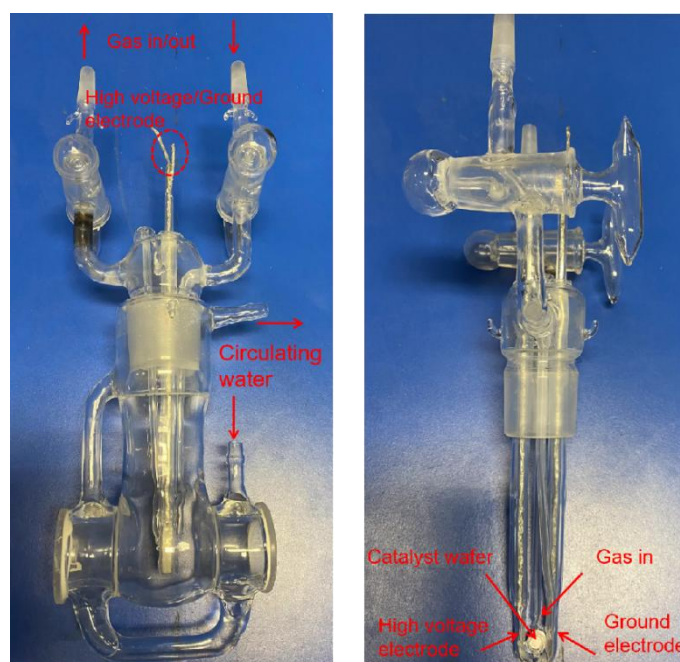


**Figure S8.** Comparison of plasma-catalytic OSRMtM employing Cu/MOR prepared by ion exchange, Cu/MOR prepared by impregnation method and Cu/SiO<sub>2</sub> catalysts prepared by impregnation method.

## 10 *In-situ* FTIR

In the *in-situ* FTIR device, the plasma was generated between the high voltage electrode and the ground electrode mounted with a 8 mm discharge gap. The catalyst wafer with an diameter of 8 mm was mounted in the discharge zone. Reaction was carried out in the FTIR reaction cell as shown in Scheme S2. Prior to the measurement, methane and argon gas were injected to purge the air for 30min. At the same time, the gasification temperature of the steam generator and the heat strip temperature were raised to 115 °C. The temperature of circulating water in the FTIR reaction cell was raised to 70 °C to avoid condensation of water vapor. The instrument parameters are set to 8  $\text{cm}^{-1}$  optical resolution and 8 scans, and the scan range was 4000-900  $\text{cm}^{-1}$ . The background was collected after the raw gas ( $\text{CH}_4/\text{Ar}/\text{H}_2\text{O}$ ) was injected for 10min. At the same time, the plasma was turned on, and the FTIR spectrometer (Nicolet iS10, Thermo Scientific) was employed to automatically collect IR signals of the species in the gas phase and on catalyst surface using an OMNIC software. The discharge power was maintained at ca. 30W, and the discharge was stopped after the reaction for 30 min.



**Scheme S2.** Schematic diagram of the *in-situ* FTIR reaction cell.

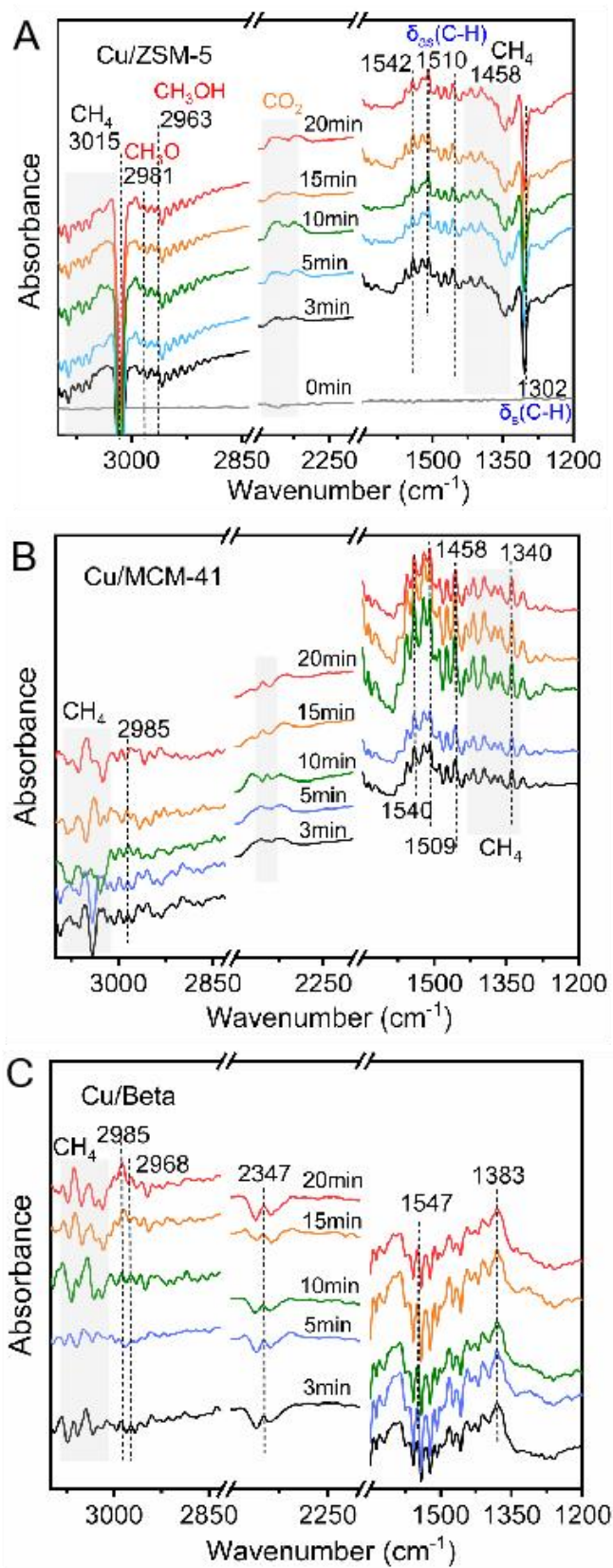


**Figure S9.** *In-situ* FTIR spectra of plasma-catalytic OSRMtM on (A) Cu/ZSM-5, (B) Cu/MCM-41 and (C) Cu/Beta.

## 11 Characterization of the spent catalysts

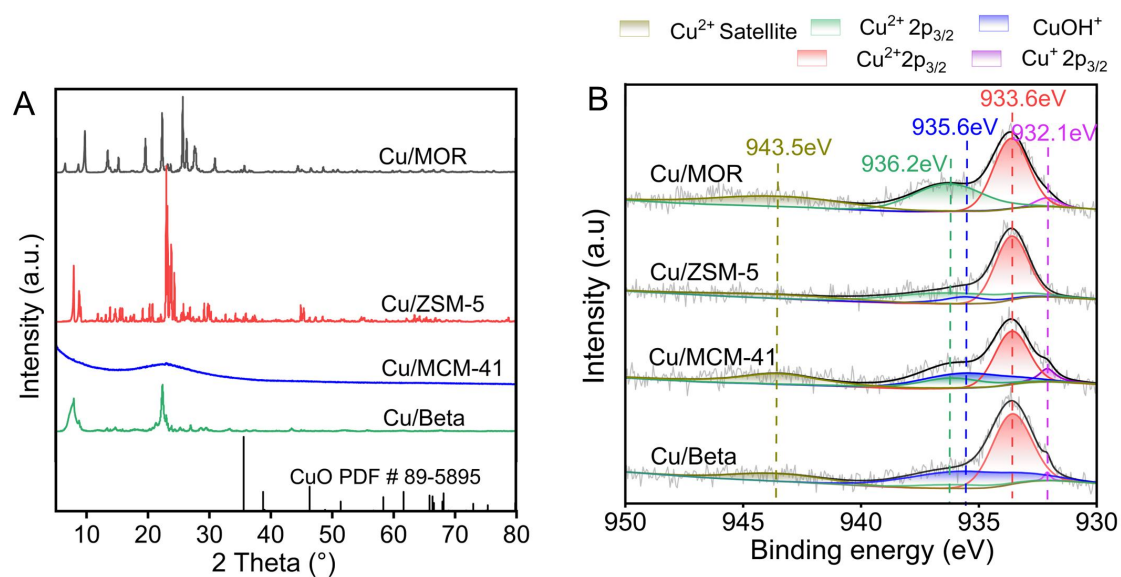


**Figure S10.** Characterization of the spent Cu/zeolite catalysts. (A) XRD patterns, (B) Cu 2P<sub>3/2</sub> XPS.

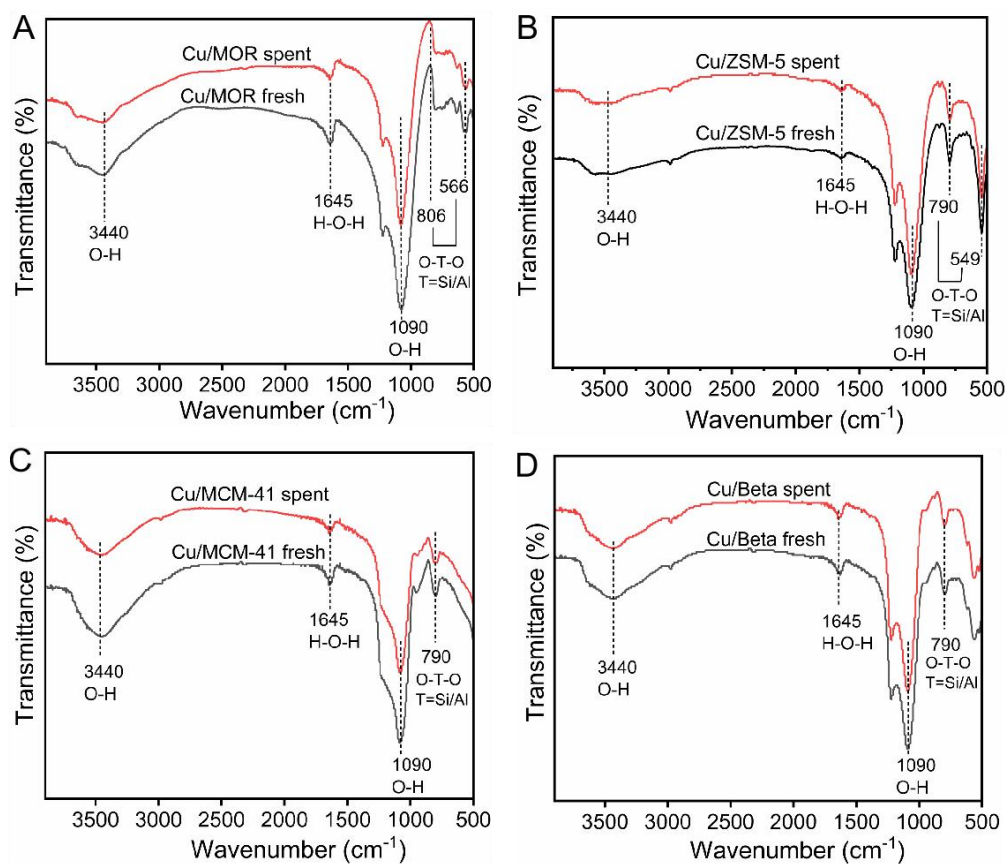


**Figure S11.** FTIR spectra of the fresh and spent Cu/zeolite catalysts. (A) Cu/MOR, (B) Cu/ZSM-5, (C) Cu/MCM-41 and (D) Cu/Beta.

## **12 *In-situ* Optical emission spectra**

A SP 2758 spectrometer (Princeton Instruments) was used to analyze the optical emission spectra of the CH<sub>4</sub>/H<sub>2</sub>O/Ar plasma with wavelength from 200 to 1100 nm (Figure 3A), aiming to diagnose active species in the CH<sub>4</sub>/H<sub>2</sub>O/Ar plasma. A 300 g·mm<sup>-1</sup> grating was used and the slit width of the spectrometer was fixed at 20 μm with an exposure time of 2 s.

## References

1. K. Okazaki, T. Kishida, K. Ogawa and T. Nozaki, *Energy Conversion and Management* 2002, **43**, 1459–1468.
2. T. Tsuchiya and S. Iizuka, *Journal of Environmental Engineering and Technology*, 2013, **2**, 35-39.
3. D. W. Larkin, L. L. Lobban and R. G. Mallinson, *Catalysis Today*, 2001, **71**, 199-210.
4. L. M. Zhou, B. Xue, U. Kogelschatz and B. Eliasson, *Plasma Chemistry and Plasma Processing*, 1998, **18**, 375-393.
5. H. Matsumoto, S. Tanabe, K. Okitsu, Y. Hayashi and S. L. Suib, *The Journal of Physical Chemistry A*, 2001, **105**, 5304-5308.
6. H. Zheng and Q. Liu, *Mathematical Problems in Engineering*, 2014, **2014**, 1-10.
7. W. Bi, Y. Tang, X. Li, C. Dai, C. Song, X. Guo and X. Ma, *Communications Chemistry*, 2022, **5**, 124.
8. Y. Tang, Y. Cui, G. Ren, K. Ma, X. Ma, C. Dai and C. Song, *Fuel Processing Technology*, 2023, **244**, 107722.
9. P. Chawdhury, Y. Wang, D. Ray, S. Mathieu, N. Wang, J. Harding, F. Bin, X. Tu and C. Subrahmanyam, *Applied Catalysis B: Environmental*, 2021, **284**, 119735.
10. A. Indarto, *Ionics*, 2014, **20**, 445-449.
11. Y. Yi, S. Li, Z. Cui, Y. Hao, Y. Zhang, L. Wang, P. Liu, X. Tu, X. Xu, H. Guo and A. Bogaerts, *Applied Catalysis B: Environmental*, 2021, **296**, 120384.
12. P. Chawdhury, D. Ray and C. Subrahmanyam, *Fuel Processing Technology*, 2018, **179**, 32-41.
13. H. Lv, X. Liu, Y. Hao and Y. Yi, *Plasma Chemistry and Plasma Processing*, 2023, **43**, 1963-1978.
14. L. Chen, X. Zhang, L. Huang and L. Lei, *Journal of Natural Gas Chemistry*, 2010, **19**, 628-637.
15. L. Chen, X. Zhang, L. Huang and L. Lei, *Chemical Engineering & Technology*, 2010, **33**, 2073-2081.
16. S. Mahammadunnisa, K. Krushnamurthy and C. Subrahmanyam, *Catalysis Today*, 2015, **256**, 102-107.